

Asymptotically Optimal Path Planning for Ground Surveillance by a Team of UAVs

Andrey V. Savkin and Hailong Huang

Abstract—This letter addresses a path planning problem for a team of mobile robots such as unmanned aerial vehicles (UAVs) patrolling a ground region for surveillance. An effective navigation algorithm is developed and proved to be asymptotically optimal in the sense that the ratio of the revisit period of the algorithm and the minimum possible revisit period converges to 1 as the area of the region tends to infinity. Illustrative examples and comparisons with an existing method show the efficiency of the developed approach.

Index Terms—Mobile robots, unmanned aerial vehicles, UAVs, aerial surveillance, sweep coverage, path planning, navigation, aerial drones, coverage control, marine surface vehicles.

I. INTRODUCTION

Mobile robots have become a popular tool for monitoring and surveillance of targets in various military and civilian applications including ground traffic surveillance, inspection of agricultural fields, infrastructure monitoring and inspection, natural disaster areas surveillance, rescue missions, and ground monitoring for security purposes. In such surveillance applications, a typical situation is that a team of flying robots such as unmanned aerial vehicles (UAVs), equipped with ground-facing cameras, monitors a ground region. One common approach to such surveillance problems is to deploy the minimum number of robots in steady positions to cover a given ground region completely, so that any point of the region is monitored by at least one robot at any time [1], [2]. Another challenging class of problems consists of scenarios where the surveillance ground region is too large for the given number of robots, therefore, all the region cannot be monitored all the time. In this case, the robots should patrol the region so that any point of the region is surveyed at some time. Such problems can be viewed as so-called sweep coverage problems of robotics where a path planning algorithm for mobile robots to visit the whole monitored area should be developed [3], [4]. As in sweep coverage problems, any point of the region is covered not all the time but periodically, a natural problem statement is to develop a navigation algorithm that minimizes the maximum revisit time or period for the whole region.

Previous research work has investigated this problem for ground robots. Most approaches first decompose the free

region and then compute a global solution. There are two popular approaches for decomposition: grid-based and cellular-based [5]. In grid-based approaches, the region is represented as a grid map, and then a spanning tree is built for path planning [6]. The main difficulty is the efficiency, which depends on the resolution of the map. The cellular decomposition splits the region into non-overlapping cells, and the widely used method is the boustrophedon decomposition [7]. This method takes some critical points on the boundary of obstacles for decomposition. Other methods such Voronoi diagram have also been used for cellular decomposition [8]. The main demerit of these approaches is the obtained cells may be unbalanced, which leads to various revisit times of the cells.

This letter addresses the revisit period minimization problem and develops an algorithm for navigating a team of UAVs so that every point of a given ground region is periodically surveyed. The result of this manuscript reminds in spirit the main result of [1] where a method for static deployment of UAVs over a ground region was proposed. We prove that the proposed algorithm is asymptotically optimal in the sense that the ratio of the revisit period of the algorithm and the minimum possible revisit period converges to 1 as the area of the ground region tends to infinity. Asymptotic optimality cannot be achieved by the aforementioned methods. The comparison with a grid-based benchmark method shows that the proposed method achieves short paths, especially for large-scale regions. Moreover, it is a construction method requiring a much lower computation load than other existing methods.

We formally state the problem in Section II. The proposed algorithm and the main result are given in Section III. Section IV contains illustrative examples and comparisons with another method. A brief conclusion is given in Section V.

II. PROBLEM STATEMENT

Let $p \in \mathbf{R}^2$ be the vector of Cartesian coordinates on the ground plane. Moreover, let \mathcal{D} be a given bounded, closed and Lebesgue measurable region [9] of the ground plane. There are n UAVs labelled $1, 2, \dots, n$ that flying over \mathcal{D} at a given altitude $a > 0$. We assume that the motion of each UAV is described by the equation

$$\dot{p}_i(t) = v_i(t) \quad (1)$$

where $p_i(t)$ is the coordinates of the projection of the current position of the UAV i to the ground plane, and $v_i(t)$ is the current UAV velocity vector. We assume that $\|v_i(t)\| \leq V$, where $V > 0$ is given, and $\|\cdot\|$ denotes the standard Euclidean vector norm. This motion model is suitable for rotary-wing

This work was supported by the Australian Research Council. Also, this work received funding from the Australian Government, via grant AUMURIB000001 associated with ONR MURI grant N00014-19-1-2571.

A.V. Savkin is with School of Electrical Engineering and Telecommunications, University of New South Wales, Sydney 2052, Australia. (E-mail: savkin@unsw.edu.au).

H. Huang is with the Department of Aeronautical and Aviation Engineering, the Hong Kong Polytechnic University, Hong Kong. (E-mail: hailong.huang@polyu.edu.hk).

UAVs, and it allows the UAVs to make sharp turns. It enables the UAVs to follow the designed paths, as they may have sharp corners as seen later. Moreover, UAVs are equipped with ground facing video cameras with a given observation angle $0 < \alpha < \pi$, which defines the visibility cone of UAVs, so that the UAV i at time t can only see points P of the ground that are inside of the circle of radius

$$r := \tan\left(\frac{\alpha}{2}\right)a \quad (2)$$

centred at $p_i(t)$, see Fig. 1.

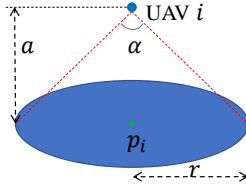


Fig. 1: The visibility cone.

Let $\mathcal{I}(P)$ be the set of all time intervals $[m, M]$ where $0 \leq m < M$, during which the point $P \in \mathcal{D}$ is not seen from any of n UAVs. Moreover, let

$$\beta(P) := \sup_{[m, M] \in \mathcal{I}(P)} (M - m), \quad \beta(\mathcal{D}) := \sup_{P \in \mathcal{D}} \beta(P). \quad (3)$$

Problem Statement: Our objective is to develop a path planning algorithm for n UAVs satisfying (1) that solves the following revisit period optimization problem

$$\beta(\mathcal{D}) \rightarrow \min. \quad (4)$$

Remark II.1. It is clear that the revisit period $\beta(\mathcal{D})$ is some measure of the quality of surveillance of the ground region \mathcal{D} by n UAVs flying over \mathcal{D} , in the sense that the smaller $\beta(\mathcal{D})$, the shorter the maximum time during which some point of \mathcal{D} is not seen by any UAV. So our objective is to navigate the UAVs to minimize $\beta(\mathcal{D})$.

III. PATH PLANNING ALGORITHM

Definition III.1. Let l be a straight line on the ground plane. A closed planar set \mathcal{E} is said to be l -convex if the intersection of any straight line parallel to l with \mathcal{E} is either empty or a single point or a closed interval, see Fig. 2.

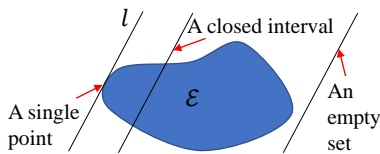


Fig. 2: Illustration of an l -convex closed planar set \mathcal{E} .

Remark III.1. Any convex set is l -convex for any l .

Assumption III.1. There exist straight lines l_1, \dots, l_n such that \mathcal{D} can be partitioned into n closed, bounded and l_i -convex regions $\mathcal{D}_i, i = 1, \dots, n$ with equal areas. Moreover, any \mathcal{D}_i has piecewise smooth boundary of length L_i .

The proposed path planning algorithm for a region \mathcal{D} satisfying Assumption III.1, consists of the following steps.

Step A1: We take l_i and \mathcal{D}_i from Assumption III.1.

Step A2: For any i , we build a sequence of straight lines parallel to l_i at the distance $2r$ between any two closest to each other lines, where r is defined by (2), see Fig. 3.

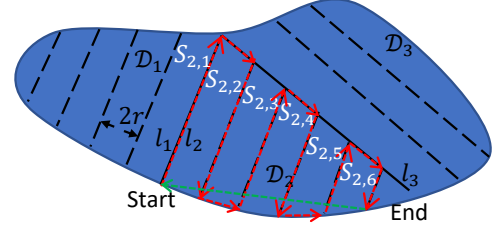


Fig. 3: Illustration of constructing the closed paths for UAVs.

Step A3: Since \mathcal{D}_i is bounded and l_i -convex, the intersection of \mathcal{D}_i with the corresponding family of parallel straight lines consists of several parallel segments $S_{i,1}, S_{i,2}, \dots, S_{i,k(i)}$ (some of them maybe single points). We start at some end of $S_{i,1}$ and move along this segment until we reach the boundary of \mathcal{D}_i . Then we move along the boundary until we reach $S_{i,2}$, and then we move along $S_{i,2}$ in the opposite direction until we reach the boundary again, see Fig. 3.

Step A4: We repeat **Step A3** again and again until we reach the end of $S_{i,k(i)}$, see Fig. 3.

Step A5: We connect the final point of our path on $S_{i,k(i)}$ with the initial point of our path on $S_{i,1}$ by some curve inside \mathcal{D}_i (if possible by a straight line). Since the length of the boundary is L_i , there always exists a path no longer than $\frac{L_i}{2}$.

Step A6: For each i , the UAV i is flying along the closed path constructed in **A1–A5** with the maximum speed V .

Notice that the algorithm **A1–A6** is close to various lawn mowing type path planning algorithms of robotics, see e.g. [10]. We will analyse optimality of the path planning algorithm **A1–A6**. Let $\gamma > 1$ be some number. Introduce the region \mathcal{D}_γ obtained from the region \mathcal{D} by the linear transformation that maps any point $P \in \mathcal{D}$ to the point $(\gamma x, \gamma y)$, see Fig. 4. So the region \mathcal{D}_γ is similar to \mathcal{D} but larger. It is also obvious that

$$A(\mathcal{D}_\gamma) = \gamma^2 A(\mathcal{D}) \quad (5)$$

where $A(\cdot)$ denotes the area of a region.

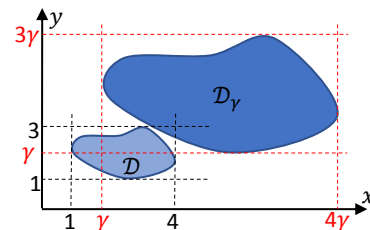


Fig. 4: Constructing region \mathcal{D}_γ from region \mathcal{D} .

Furthermore, consider some family $\mathcal{F}(\gamma)$ of paths constructed by **Steps A1–A6** over \mathcal{D}_γ for all $\gamma > 1$. Let $\hat{\beta}(\gamma)$ be the value of $\beta(\mathcal{D}_\gamma)$ defined by (3) with UAVs flying along

the paths $\mathcal{F}(\gamma)$. Let $\beta_0(\gamma)$ be the minimal possible value of $\beta(\mathcal{D}_\gamma)$ for all flying paths of UAVs over the ground region \mathcal{D}_γ . It is clear that since the region \mathcal{D}_γ increases as γ increases, both $\hat{\beta}(\gamma)$ and $\beta_0(\gamma)$ tend to infinity as γ tends to infinity.

Definition III.2. A family $\mathcal{F}(\gamma)$ of UAV paths in the regions \mathcal{D}_γ is said to be asymptotically optimal, if

$$\lim_{\gamma \rightarrow \infty} \frac{\hat{\beta}(\gamma)}{\beta_0(\gamma)} = 1. \quad (6)$$

In other words, path planning is asymptotically optimal, if as the ground region becomes larger, the quality of surveillance with these paths defined by (3) becomes close to the best possible quality of surveillance.

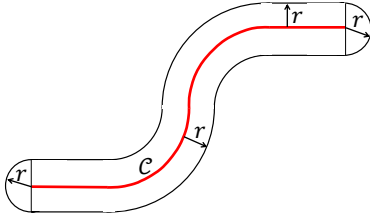


Fig. 5: r -neighbourhood of curve \mathcal{C} (set S).

Theorem III.1. Let $\mathcal{F}(\gamma)$ be the family of UAVs paths in the regions \mathcal{D}_γ constructed by the path planning algorithm **A1–A6**. Then $\mathcal{F}(\gamma)$ is asymptotically optimal. Moreover,

$$\lim_{\gamma \rightarrow \infty} \frac{\hat{\beta}(\gamma)}{\gamma^2} = \frac{A(\mathcal{D})}{2nVr} \quad (7)$$

where $A(\cdot)$ denotes the area of a region.

Proof. First we prove that the family of UAVs paths $\mathcal{F}(\gamma)$ constructed by **A1–A6** satisfies (7). Indeed, let $H_i(\gamma)$ be the sum of the lengths of all segments parallel straight lines built in $\mathcal{D}_{i\gamma}$ in **Step A2**. Then it is obvious that

$$\lim_{\gamma \rightarrow \infty} \frac{A(\mathcal{D}_{i\gamma})}{2rH_i(\gamma)} = 1. \quad (8)$$

Since $A(\mathcal{D}_{i\gamma}) = \gamma^2 A(\mathcal{D}_i) = \frac{\gamma^2 A(\mathcal{D})}{n}$, (8) implies that

$$\lim_{\gamma \rightarrow \infty} \frac{\gamma^2 A(\mathcal{D})}{2rnH_i(\gamma)} = 1. \quad (9)$$

Furthermore, it is obvious that the length $T_i(\gamma)$ of the closed UAV trajectory constructed in $\mathcal{D}_{i\gamma}$ by **A1–A6** satisfies $H_i(\gamma) < T_i(\gamma) \leq H_i(\gamma) + \frac{3\gamma L_i}{2}$. Since the UAVs are moving with the maximum speed V , this and (9) imply (7). Now we prove that for any family of paths,

$$\lim_{\gamma \rightarrow \infty} \frac{\beta(\gamma)}{\gamma^2} \geq \frac{A(\mathcal{D})}{2nVr} \quad (10)$$

Indeed, consider any curve \mathcal{C} of length L and the set S of all points at the distance r or less from some point of this curve, see Fig. 5. Then the area of this set satisfies $A(S) \leq 2Lr + \pi r^2$. This implies that the minimum length $F(\gamma)$ of curves in $\mathcal{D}(\gamma)$

with the property that for any point $\mathcal{D}(\gamma)$ there exists a point of curves at the distance r or less, satisfies

$$\lim_{\gamma \rightarrow \infty} \frac{\gamma^2 A(\mathcal{D})}{2rF(\gamma)} \geq 1. \quad (11)$$

Since we have n UAVs and their maximum speed is V , (11) implies (10). This completes the proof of Theorem III.1. \square

IV. SIMULATIONS

In this section, we show the effectiveness of the proposed approach via computer simulations.

We consider using rotary-wing UAVs to survey a given region \mathcal{D} . Here, we do not consider where the UAVs start. Though their starting points impact the time to complete the first trip, they do not influence the revisit time of the later rounds. The first task is to find the set of straight lines satisfying Assumption III.1. Our method to find this set of lines is stated as follows. Given \mathcal{D} , we first find a line l'_1 such that \mathcal{D} is l'_1 -convex and l'_1 is tangent to \mathcal{D} ; see Fig. 6. Then, we move l'_1 in parallel inwards \mathcal{D} to get another line l_1 , such that the sub-region of \mathcal{D} between l'_1 and l_1 , denoted by \mathcal{D}_1 , satisfies $A(\mathcal{D}_1) = \frac{1}{n} A(\mathcal{D})$. Now, we have the first line l_1 . Let \mathcal{D}_{remain} denote the remaining sub-region after removing \mathcal{D}_1 from \mathcal{D} , i.e., $\mathcal{D}_{remain} = \mathcal{D} / \mathcal{D}_1$. We then find a line l'_2 such that \mathcal{D}_{remain} is l'_2 -convex. We move l'_2 in parallel inwards \mathcal{D}_{remain} to get l_2 ; see Fig. 6. We repeat this until \mathcal{D} is divided into n sub-regions with equal areas. A simplified version of the above method is stated as follows. After having l_1 , instead of finding another line l'_2 , we move l_1 further to get l_2 , such that 1) l_2 is parallel to l_1 and 2) the area of the sub-region of \mathcal{D} between l_1 and l_2 is $\frac{1}{n} A(\mathcal{D})$. By this simplified method, we obtain a set of parallel straight lines. Illustrative examples of the simplified method is shown in Fig. 7, where $n = 3$, $\alpha = \frac{\pi}{2}$ and $a = 10$ m. We show the cases with $\gamma = 1$ and $\gamma = 2$, respectively. These examples demonstrate how the paths are generated according to the proposed method.

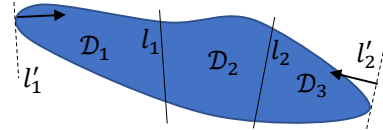


Fig. 6: Constructing a set of straight lines to partition \mathcal{D} into n sub-regions with equal areas.

We make a comparison with a benchmark method [3]. This method consists of three steps. Firstly, it partitions the area of interest, which is similar to our method. Then, it grids each sub-area by squares whose edge length is $2r$. The grids overlapping with the sub-area are considered as waypoints. Finally, for each sub-area, it solves a travelling salesman problem (TSP) using the Generic Algorithm (GA) to construct a tour that visits each of the waypoints once. We use the MATLAB embedded function to solve the problems. Using the same area as above, the obtained UAVs' trajectories by the benchmark method are shown in Fig. 8, where $n = 3$, and γ takes 1 and 2, respectively.

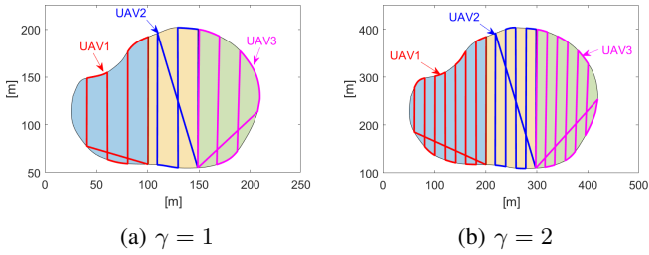


Fig. 7: Trajectories constructed by the proposed approach.

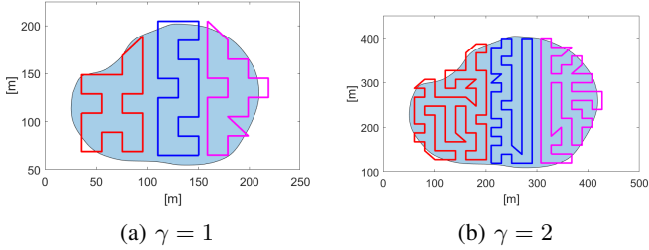


Fig. 8: Trajectories constructed by the benchmark method [3].

We now compare simulation result with Theorem III.1. Using the same parameters of α and a , we consider different values of γ . As seen from Fig. 9a, with the increase of γ (from 1 to 30), the value of $\frac{\hat{\beta}(\gamma)}{\gamma^2}$ decreases, and it tends to be the optimal value of $\frac{A(\mathcal{D})}{2nVr}$, where $V = 1$ m/s and $r = 10$ m (computed by (2)). Simulation results for other values of n are also shown in Fig. 9a. We have also applied the proposed method to areas with different shapes, and similar results are obtained. These results are in accordance with Theorem III.1.

We also apply the benchmark to cases with larger γ (up to 10) and compare it with the proposed method. With the increase of γ , the area \mathcal{D}_γ increases, so more grids are needed to fully cover \mathcal{D}_γ . As solving TSP instances is computationally heavy with respect to the number of points, γ takes up to 10 for the benchmark. As seen from Fig. 9a, for small values of γ , the benchmark achieves better results. The reason is that in our method when γ is small, the connection between the starting point and ending point, which is constructed according to **Step A5**, takes a relatively large part of a whole path, e.g., see the trajectories of UAV2 in Fig. 7. When γ is small, it is easy to optimally solve the TSP instances. For large γ , the proposed method outperforms the benchmark, as it is difficult for GA to search the optimal solution under a given number of iterations. Besides, the proposed method is more computationally efficient. It only takes a few seconds to complete (see Fig. 9b), while the benchmark can take several minutes. Moreover, the computational time of our method is not sensitive to γ but only to n . Because partitioning the region takes a relatively long time in finding a set of lines l_1, l_2, \dots, l_n , while constructing a trajectory only needs to move a line l_i in parallel to obtain other straight lines. In contrast, the computation time of the benchmark significantly depends on γ , as larger γ means more grids to visit.

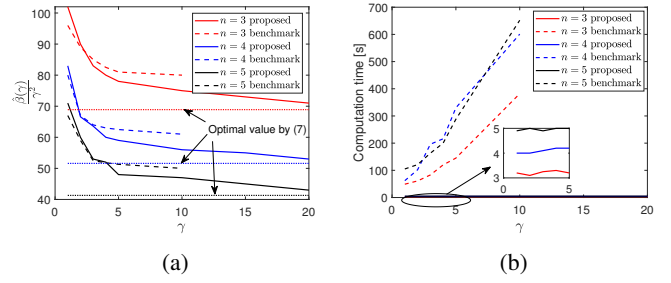


Fig. 9: Comparison with the benchmark method. (a) $\frac{\hat{\beta}(\gamma)}{\gamma^2}$ versus γ . (b) Computation time versus γ .

V. CONCLUSION

A problem of UAV navigation for surveillance was studied. In this problem, UAVs equipped with ground-facing cameras are navigated over a ground region to periodically monitor every point of the region. An efficient navigation algorithm was developed. The developed algorithm is asymptotically optimal in the sense that the revisit period of the algorithm is getting close to the optimal revisit period as the size of the ground region tends to infinity. Illustrative examples and comparisons with another approach showed the efficiency of the proposed method. It is worth pointing out that the proposed method is not restricted to UAVs but also works for other types of mobile robots, such as marine surface vehicles, when the assumptions mentioned in the paper are met. A limitation is that the current result is only suitable for flat regions. For uneven terrains, the designed paths may not guarantee full coverage, and this is an interesting direction for future research. Another interesting direction is to study the case with heterogeneous mobile robots that can move at different speeds.

REFERENCES

- [1] A. V. Savkin and H. Huang, "Asymptotically optimal deployment of drones for surveillance and monitoring," *Sensors*, vol. 19, no. 9, p. 2068, 2019.
- [2] A. V. Savkin and H. Huang, "A method for optimized deployment of a network of surveillance aerial drones," *IEEE Systems Journal*, vol. 13, no. 4, pp. 4474–4477, 2019.
- [3] S. Ann, Y. Kim, and J. Ahn, "Area allocation algorithm for multiple UAVs area coverage based on clustering and graph method," *IFAC-PapersOnLine*, vol. 48, no. 9, pp. 204–209, 2015.
- [4] X. Gao, J. Fan, F. Wu, and G. Chen, "Approximation algorithms for sweep coverage problem with multiple mobile sensors," *IEEE/ACM Transactions on Networking*, vol. 26, no. 2, pp. 990–1003, 2018.
- [5] N. Karapetyan, K. Benson, C. McKinney, P. Taslakian, and I. Rekleitis, "Efficient multi-robot coverage of a known environment," in *2017 IEEE/RSJ International Conference on Intelligent Robots and Systems (IROS)*. IEEE, 2017, pp. 1846–1852.
- [6] Y. Gabriely and E. Rimon, "Spanning-tree based coverage of continuous areas by a mobile robot," *Annals of mathematics and artificial intelligence*, vol. 31, no. 1, pp. 77–98, 2001.
- [7] H. Choset, "Coverage of known spaces: The boustrophedon cellular decomposition," *Autonomous Robots*, vol. 9, no. 3, pp. 247–253, 2000.
- [8] A. Yazici, G. Kirlik, O. Parlaktuna, and A. Sipahioğlu, "A dynamic path planning approach for multirobot sensor-based coverage considering energy constraints," *IEEE Transactions on Cybernetics*, vol. 44, no. 3, pp. 305–314, 2014.
- [9] A. N. Kolmogorov and S. V. Fomin, *Introductory real analysis*. New York: Dover, 1975.
- [10] Y. Choi, Y. Choi, S. Briceno, and D. N. Mavris, "Energy-constrained multi-UAV coverage path planning for an aerial imagery mission using column generation," *Journal of Intelligent & Robotic Systems*, vol. 97, no. 1, pp. 125–139, 2020.